20. C. Emiliani, *Bull. Geol. Soc. Amer.* **75**, 129 (1964).
21. W. L. Donn, W. R. Farrand, M. Ewing, *J. Geol.* **70**, 206 (1964).
22. A. S. Merrill, K. O. Emery, Meyer Rubin, *Science* **147**, 398 (1965).
23. J. C. Medcof, A. H. Clarke, Jr., J. S. Erskine, *J. Fish. Res. Bd. Canada* **22** (2), 631 (1965).
24. J. R. Curray, in *The Quaternary of the United States*, H. E. Wright and D. G. Frey, Eds. (Princeton Univ. Press, Princeton, N.J., 1965), p. 723.
25. F. C. Whitmore, Jr., K. O. Emery, H. B. S. Cooke, D. J. P. Swift, *Science* **156**, 1477 (1967).
26. K. O. Emery and R. L. Edwards, *Amer. Antiquity* **31**, 733 (1966).
27. W. S. Newman, unpublished thesis, New York Univ. (1966); W. S. Newman and R. W. Fairbridge, in *Proc. First Nat. Coastal and Shallow Water Res. Conf.* (National Science Foundation and Office of Naval Research, Tallahassee, Florida, 1962, p. 188.
28. W. Harrison, R. J. Malloy, G. A. Rusnak, J. Terasmae, *J. Geol.* **73**, 201 (1965).
29. K. O. Emery, in preparation.
30. M. B. Davis and E. S. Deevey, *Science* **145**, 1293 (1964).
31. W. F. Libby, *Radiocarbon Dating* (Univ. of Chicago Press, Chicago, ed. 2, 1955).
32. P. Butler, *Ecology* **40**, 735 (1959).
33. C. A. Kaye and E. S. Barghoorn, *Bull. Geol. Soc. Amer.* **75**, 63 (1964).
34. G. W. Barendsen, E. S. Deevey, L. J. Gralenski, *Science* **126**, 908 (1957); E. S. Deevey, L. J. Gralenski, V. Hoffren, *Amer. J. Sci. Radiocarbon Suppl.* **1**, 144 (1959); Deevey (personal communication, April 1967) now accepts the date 15,090 years before the present for Totoket Bog.
35. C. R. Groot and J. J. Groot, *Amer. J. Sci.* **262**, 488 (1964).
36. E. S. Deevey, Jr., *Amer. J. Sci.* **246**, 329 (1948).
37. W. S. Benninghoff, *Phillips Acad. Peabody Foundation, Archaeol. Papers* **2**, 96 (1942).
38. E. A. Stanley, *Deep-Sea Res.* **13**, 921 (1966).
39. J. G. Ogden, III, *Amer. J. Sci.* **261**, 344 (1963).
40. E. B. Leopold, *Proc. Nat. Acad. Sci. U.S.* **52**, 863 (1956).
41. E. Uchupi, *Misc. Geol. Invest. Map I-451* (U.S. Geological Survey, Washington, D.C., 1965).
42. M. B. Davis, in *The Quaternary of the United States*, H. E. Wright and D. G. Frey, Eds. (Princeton Univ. Press, Princeton, N.J., 1965), p. 377.
43. Appreciation is due Captain Norman Lepire of New Bedford, Massachusetts, for several samples of peat and oyster shells, and to the U.S. Geological Survey through its support by contract 8358 to the Woods Hole Oceanographic Institution. Contribution No. 1968 of the Woods Hole Oceanographic Institution. Publication approved by the director, U.S. Geological Survey.

23 June 1967 ■

Radium-226 and Radon-222: Concentration in Atlantic and Pacific Oceans

Abstract. *Measurements of radon-222 in seawater suggest the following. The radium-226 content of surface water in both the Atlantic and Pacific oceans is uniformly close to about 4 ×* 10^{-14} *gram per liter. The deep Pacific has a concentration of radium-226 that is four times higher and the deep Atlantic a concentration twice as high as that of the surface. These distribution profiles can be explained by the same particle-settling rate for radium-226 from surface to depth for the two oceans and by a threefold longer residence time of water in the deep Pacific than in the deep Atlantic. The vertical distribution of the deficiency of radon-222 in the surface water of the northwest Pacific Ocean suggests a coefficient of vertical eddy diffusion as high as 120 square centimeters per second and a gas-exchange rate for carbon dioxide in surface water between 14 and 60 moles per square meter per year. Vertical profiles of the excess of radon-222 in near-bottom water of the South Atlantic give coefficients of vertical eddy diffusion ranging from 1.5 to more than 50 square centimeters per second.*

Shipboard analysis of the concentration of radon gas in samples of seawater offers three important types of information: (i) the distribution of Ra^{226} in the world ocean, (ii) the exchange rates of gases across the air-sea interface, and (iii) the rates of vertical mixing near the surface and near the bottom of the ocean. Briefly, Rn^{222} (half-life, 3.85 days) is produced in seawater by the decay of its parent Ra^{226} (half-life, 1600 years). Well away from the air-sea and sediment-sea interfaces, the rate of radioactive decay of radon is equal to that of its parent radium.

Thus, a measurement of the radon content of such a water sample is a measurement of its radium content. As the radon content of the atmosphere is negligible, compared to that in surface seawater, radon continually escapes from the sea. By analyzing the vertical distribution of radon deficiency in the surface ocean it is possible to determine the rates of both vertical mixing and gas exchange. Water in the pores of deep-sea sediments contains 10^4 to 10^5 times more radon than the overlying seawater. Hence, radon diffuses from the sediment into the sea. The vertical distribution of excess radon in near-bottom water provides an index of the rate of vertical mixing. This report extends an earlier study (*1*) by presenting positive results for each of these applications.

Radon was extracted from 20 to 40 liters of seawater by circulating He gas in a closed system at the rate of 2 liter/min for 90 minutes. The condensable gases (including radon) were continuously collected in traps cooled with liquid air. The radon was then separated from CO_2 and H_2O by circulating the condensed gas through ascarite. Next it was quantitatively transferred to a 30-cm^3 scintillation cell where the count of its α-particles was determined. Overall recovery yields averaged 90 percent; accuracy of the measurements is about ±10 percent. Details of the procedure have already been published (*1*).

Although our results change neither the average content of radium content in the ocean nor the broad picture of its distribution from that given by previous workers (*2, 3*), they do show far less scatter and suggest that radium is uniformly mixed throughout a given water mass. The radium content of surface water in both the Atlantic and Pacific oceans is 4 × 10^{-14} g/liter (Table 1 and Fig. 1). In both oceans a smooth increase in radium takes place downward through the main thermocline; in the Pacific the increase is fourfold (to 16 × 10^{-14} g/liter) and in the North Atlantic, twofold (to 8 × 10^{-14} g/liter).

Two explanations have been offered for the deficiency of radium in surface relative to deep water. Koczy (*2*) suggested that it reflected radioactive decay during the period in which surface water was isolated from the deep sea. The mixing rates required by this hypothesis are an order of magnitude lower than those that explain the vertical distribution of natural radiocarbon [see Broecker (*4*)]. Chow and Goldberg (*5*) have suggested that the deficiency is generated in much the same way as that for silicon and phosphorus. Radium in surface water is fixed onto particulate matter that sinks to the deep ocean where the radium redissolves. Their demonstration that, in the Pacific, barium shows a fourfold enrichment in deep relative to surface water strongly supports this alternate hypothesis.

Despite the difference in the deep-to-surface anomaly for radium in the two oceans the same particulate extraction rate, *I*, is required for both. Material balance requires that $I = R(C_D - C_S)$. The rate of transfer, *R*, of water across the main thermocline is given by

$$R = \frac{\bar{h}}{t_M(C_D' - C_S'/C_D')}$$

where $\bar{h}$ is the mean depth of the ocean; C_D' and C_S' are the C^{14}/C^{12} ratios in the deep and surface ocean;

Table 1. Concentrations of Ra^{226} and Rn^{222} in the oceans. *A*, specific activity.

Sample No.	Depth (m)	Position		Sample volume (liters)	Ra^{226} (10^{-14} g/liter)	$\frac{A_{Rn^{222}}}{A_{Ra^{226}}}$
		Latitude	Longitude			
		Northwest Pacific Ocean (Vema-21, *leg between Hawaii to Tokyo*)				
29	150	28°47′N	158°50′E	~ 39	3.7 ± 0.1	*
26	300	27°05′N	166°04′E	~ 39	3.8 ± .1	*
20	450	25°31′N	172°45′E	~ 39	3.7 ± .2	*
17	600	24°58′N	176°16′E	~ 39	5.3 ± .2	*
27	600	27°54′N	162°31′E	~ 39	5.0 ± .2	*
23	800	26°26′N	169°02′E	~ 39	6.9 ± .4	*
5	1000	22°14′N	165°14′W	~ 39	9.1 ± .3	*
22	1250	26°26′N	169°02′E	~ 39	10.9 ± .4	*
24	1500	26°26′N	169°02′E	~ 39	11.8 ± .4	*
19	2000	25°31′N	172°45′E	~ 39	12.9 ± .2	*
7	3000	22°51′N	169°41′W	~ 39	14.2 ± .2	*
15	4000	24°31′N	179°21′E	~ 39	16.1 ± .4	*
10	4600	23°27′N	173°14′W	~ 39	16.1 ± .4	*
25	5000	27°05′N	166°04′E	~ 39	15.1 ± .3	*
		East Equatorial Pacific Ocean (Conrad-10, *leg between Panama to Monzanillo*)				
48	200	02°48′N	113°36′W	36	4.2 ± 0.3	*
45	400	02°41′S	115°54.5′W	36	5.0 ± .3	*
47	720	01°19.6′N	114°50.5′W	36	5.6 ± .3	*
39	1060	01°49′N	91°14′W	36	10.0 ± .4	*
41	1510	05°36′N	96°10′W	36	10.9 ± .4	*
49	2500	03°33′N	113°12.5′W	36	12.8 ± .4	*
50	3100	06°50′N	110°27′W	36	13.7 ± .4	*
37†	3230	03°51.5′N	85°57.5′W	36	14.2 ± .5	1.82 ± 0.07
47†	3790	01°19.6′N	114°50.5′W	18	15.6 ± .8	1.56 ± .09
46†	4270	02°41′S	115°54.5′W	18	15.6 ± .8	1.66 ± .09
		Northwest Atlantic Ocean (Conrad-10, *leg between Bermuda to Jamaica*)				
9S	0	24°47.2′N	54°59.5′W	36	4.0 ± 0.3	0.65 ± 0.05
9	200	24°47.2′N	54°59.5′W	36	4.1 ± .3	*
8	530	25°31.5′N	55°14.5′W	36	4.0 ± .3	*
7	1070	25°10.8′N	56°06.5′W	36	5.2 ± .3	*
11	2250	21°44.2′N	61°27.8′W	36	6.2 ± .3	*
10	3290	22°50′N	57°52.3′W	36	7.3 ± .3	*
3	4820	29°46′N	62°26′W	36	8.1 ± .4	*
5	5110	26°25.8′N	58°37.8′W	36	9.0 ± .4	*
12†	5600	21°44.2′N	61°27.8′W	36	8.1 ± .4	1.64 ± 0.09

* Assumed to be unity. † Samples taken 22 m above the sea bottom.

Table 2. Concentrations of Ra^{226}-Rn^{222} in near-surface water from the Northwest Pacific Ocean (*Vema*-21, leg between Hawaii to Tokyo). *A*, specific activity. Radon concentrations are given in radium equivalents.

Sample No.	Depth (m)	Position		Sample volume (liters)	Rn^{222} (10^{-14} g/liter)	$\left(\frac{A_{Rn^{222}}}{A_{Ra^{226}}}\right)^*$
		Latitude	Longitude			
1	Surface	20°51′N	158°09′W	~ 39	1.9 ± 0.1	0.48
3	Surface	21°36′N	161°26′W	~ 39	2.1 ± .2	.54
8	Surface	22°51′N	169°41′W	~ 39	1.6 ± .2	.41
13	Surface	24°31′N	179°21′E	~ 39	2.5 ± .2	.64
14	Surface	24°31′N	179°21′E	~ 39	2.2 ± .2	.56
16	Surface	24°58′N	176°16′E	~ 39	3.1 ± .1	.80
18	Surface	25°31′N	172°45′E	~ 39	1.9 ± .2	.48
21	Surface	26°26′N	169°02′E	~ 39	2.1 ± .1	.54
28	Surface	28°47′N	158°50′E	~ 39	2.0 ± .1	.51
30	Surface	29°28′N	154°36′E	~ 39	2.1 ± .1	.54
31	Surface	29°51′N	150°58′E	~ 39	2.0 ± .1	.51
32	Surface	30°04′N	147°41′E	~ 39	2.2 ± .2	.56
33	Surface	30°25′N	144°30′E	~ 39	1.9 ± .1	.48
2	25	20°51′N	158°09′W	~ 39	2.5 ± .2	.65
4	25	22°14′N	165°14′W	~ 39	2.8 ± .2	.72
11	25	23°27′N	173°14′W	~ 39	2.5 ± .2	.65
12	75	23°58′N	176°51′W	~ 39	3.0 ± .1	.77
29	150	28°47′N	158°50′E	~ 39	3.7 ± .1	1.95
26	300	27°05′N	166°04′E	~ 39	3.8 ± .2	1.98

* Assuming Ra^{226} is 3.9×10^{-14} g of radium per liter.

and t_M, the mean life of radiocarbon (that is, 8040 years).

$$I_P/I_A = [(C_D - C_S)_P/(C_D - C_S)_A] \times [(1 - C_S'/C_D)_A/(1 - C_S'/C_D')_P]$$

As shown above $C_D - C_S$ is 12×10^{-14} g/liter for the Pacific, and for $\times 10^{-14}$ g/liter for the Atlantic. Radiocarbon data (*4*, *6*) yields C_S'/C_D' of approximately 0.85 for the Pacific and 0.95 for the Atlantic, hence

$$I_D/I_A = [(12 \times 10^{-14})/(4 \times 10^{-14})] \times [(1 - 0.95)/(1 - 0.85)] \cong 1$$

Therefore, the threefold longer residence time of water in the deep Pacific allows three times more radium to accumulate.

In this calculation the difference in concentration of radium generated by radioactive decay was neglected. If the mixing rates based on radiocarbon data are valid, then the decay of radium introduces only a 12 percent difference in its concentration between deep and surface water of the Pacific. The fact that, despite its shorter half-life, radium is predicted to show a smaller decay effect than radiocarbon results from its addition to the deep rather than the surface ocean (the deep ocean has a volume roughly 10 times greater than the surface ocean).

The equality of the concentrations of radium between the surface waters of the two oceans may have significance to the problem of interocean mixing. Unless it is a coincidence, it suggests that the surface waters of the Atlantic and Pacific intermix with each other more frequently than they intermix with the underlying deep water masses.

Finally, there is no evidence for any significant gradient in radium away from the sediment interface. Within the limits of error, our measurements indicate that the radium content of the deep sea is constant below 3000 m. Any gradient that is present probably reflects the same phenomena that produce salinity and temperature gradients [see Munk (*7*)]. To gain any further information from radium would require a knowledge of the vertical distribution of the resolution of falling particles. At the present time we do not even know the nature of these particles.

The next step in understanding the distribution of radium in the sea requires the precise measurement of the ratio of Ra^{226} to barium. If these two elements have identical chemistry, these ratios can be used in the same manner as C^{14}/C or Si^{32}/S ratios. As shown by Lal *et al.* (*8*) transthermocline mixing rates (that is, deep water residence times) calculated from such ratios are independent of the effects of downward particulate transport.

A series of 13 measurements made on surface ocean water (depth 1 m) between Hawaii and Japan (Table 2) clearly demonstrate that a significant amount of radon escapes to the atmosphere. As shown in Fig. 2, the radon concentration in surface water averages 0.54 of that in water from 100 to 300 m. Three measurements from 25 m average 0.68 in the equilibrium value and one measurement from 75 m, 0.77. The depth at which the anomaly reaches one-half its surface value is thus about 75 m. The seas were calm during the entire period of these measurements; the wind force averaged 1 to 2 and did not exceed 4; and the seasonal thermocline averaged 25 m.

Table 3. Concentration of Ra^{226}–Rn^{222} in near-bottom water from the South Atlantic Ocean (*Conrad*-11). All samples of water were 19 liters. Numerals in parentheses are assumed values. Radon contrations are given in radium equivalents.

Sample No.	Distance above bottom (m)	Position		Rn^{222} (10^{-14} g/liter)	Ra^{226} (10^{-14} g/liter)
		Latitude	Longitude		
R1-A	10	22°47′S	32°37′W	40.1 ± 2	7.1 ± 0.5
R1-B	17	22°47′S	32°37′W	22.0 ± 1	7.3 ± .5
R1-C	24	22°47′S	32°37′W	14.1 ± 0.7	7.3 ± .5
R1-D	31	22°47′S	32°37′W	8.0 ± .5	6.6 ± .5
R3-A	5	39°04′S	52°41′W	20.7 ± 1	(7)
R3-B	12	39°04′S	52°41′W	20.9 ± 1	(7)
R3-C	19	39°04′S	52°41′W	20.0 ± 1	(7)
R3-D	26	39°04′S	52°41′W	16.5 ± 0.8	(7)
R4-A	9	47°02′S	43°41′W	21.6 ± 1	(7)
R4-B	18	47°02′S	43°41′W	18.2 ± 1	(7)
R4-C	26	47°02′S	43°41′W	17.0 ± 0.8	(7)
R4-D	1050	47°02′S	43°41′W	6.6 ± .5	(7)

As previously shown (*1*), the fraction of equilibrium, f_x, between radon and its parent radium at any depth, x, below the sea surface is given by

$$f_x = \frac{C_x}{C_{\text{equil}}} = \frac{1}{D_M + Z\sqrt{\lambda D_E}}\left[D_M \exp\left(-x\sqrt{\frac{\lambda}{D_E}}\right) + Z\sqrt{\lambda D_E}\right]$$

where Z is the thickness of a hypothetical boundary layer through which gases must pass by molecular diffusion; D_E, the coefficient of molecular diffusion; D_M, the apparent coefficient of vertical eddy mixing; and λ, the decay constant for radon. If $x_{1/2}$ is defined as the depth at which the radon anomaly becomes half of that at the surface, that is, where $f_x = [(f_0 + 1)/2]$

$$D_E = \left(\frac{x_{\frac{1}{2}}}{0.693}\right)^2 \lambda$$

If $x_{1/2}$ is 7.50×10^3 cm and λ is 2.1×10^{-6} second, D_E turns out to be 120 cm^2/sec.

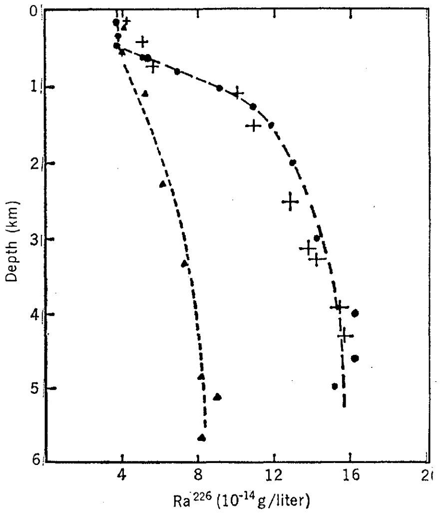

Fig. 1. The vertical distribution of Ra^{226} in the oceans. ●, Northwest Pacific Ocean; +, east equatorial Pacific; and ▲, northwest Atlantic Ocean.

The rate of exchange, R, of CO_2 gas will be given by

$$R = [D_M(CO_2)]/Z = D_M P_{CO_2} C_S')/Z$$

Since for $x = 0$

$$f_0 = \left(1 + \frac{D_M}{Z\sqrt{\lambda D_E}}\right)^{-1}$$

we have

$$R = P_{CO_2} C_S' \sqrt{\lambda D_E}\,(1 - f_0)/f_0$$

Finally, writing D_M in terms of $x_{1/2}$

$$R = [(P_{CO_2} C_S' x_{\frac{1}{2}} \lambda)/0.693] \times [(1 - f_0)/f_0]$$

The partial pressure in the atmosphere over the ocean and in mid-latitude seawater is about 3.2×10^{-4} atm. The solubility of CO_2 in seawater at 25°C is 30 mole m^{-3} atm^{-1} and λ is 66 $year^{-1}$. If $x_{1/2}$ is 75 m and f_0 is 0.54, R turns out to be 60 mole m^{-2} $year^{-1}$.

Although similar in magnitude, this result is about four times larger than the average demanded to replenish the radiocarbon undergoing radioactive decay in the sea (4).

The CO_2 exchange rate can be calculated in another way. Instead of assuming an exponential drop-off with depth, let us assume that the deficient zone lies above the seasonal thermocline and is roughly uniform over this interval. Taking the depth to the seasonal thermocline to be $\hbar$, we have

$$R = P_{CO_2} C_S' \hbar \lambda [(1 - f_0)/f_0]$$

Since $\hbar$ averages 25 m (compared to $x_{1/2}/0.693$ = 108 m), R becomes 14 mole m^{-2} $year^{-1}$, a value consistent with the distribution of natural C^{14}. This question cannot be resolved until detailed vertical profiles of the radon deficiency have been obtained.

The last column in Table 1 proves our previous prediction that easily measured excesses of radon exist in near-bottom waters. In these samples excesses ranging from 5 to 12 × 10^{-14} gram equivalent of Ra^{226} per liter were found 25 m above the sea floor [with the use of the 200-liter sampler developed by Gerard *et al.* (*9*)]. In order to obtain bottom profiles, four 30-liter Niskin samplers (Von Dorn type) were placed at 7-m intervals on the camera wire and triggered from the surface by messenger. The results (see Table 3) show that, as expected, the excess decreases away from the bottom.

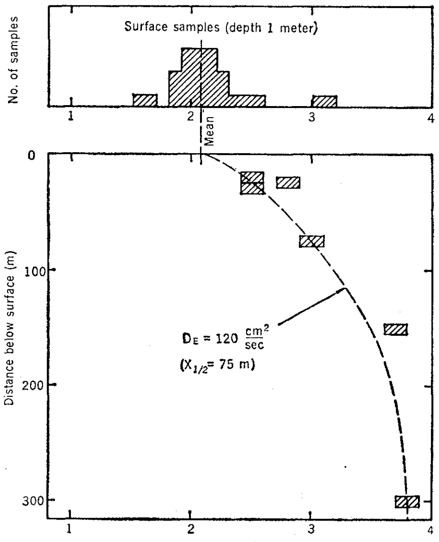

Fig. 2. The vertical distribution of Rn^{222} in surface waters of the northwest Pacific.

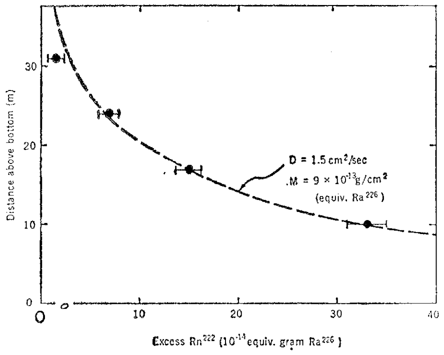

Fig. 3. Excess Rn^{222} as a function of distance above the sea bottom in the South Atlantic at 22°47′S, 32°37′W.

In our previous report it was shown that the following relation existed between the radon excess, $C_x{}^*$, and the distance from the bottom.

$$C_x{}^* = M\sqrt{\frac{\lambda}{D_E}}\ \exp\left(-x\sqrt{\lambda/D_E}\right)$$

where M is the standing crop of radon lost by the sediments, and λ and D_E are as defined above. Data for the profile 23°S, 33°W in the South Atlantic are plotted in Fig. 3. The points can be fit by the theoretical equation if D_E is 1.5 cm^2/sec and M is 9×10^{-13} gram equivalent of Ra^{226} per liter. As previously published (*1*) measurements of radon leakage from the tops of trigger-weight cores yield standing crops of from 1.5 to 35×10^{-13} gram equivalent of Ra^{226} per square centimeter. This amount of radon is also what would be expected from molecular diffusion from the radon-rich pore water [see (*1*)].

For the other two profiles roughly the same standing crop of excess radon is required, but the eddy diffusion rate must be about 30 times higher (that is, ~50 cm^2/sec). Hence the study of the distribution of excess radon near the ocean bottom will prove to be a powerful tool in determining rates of vertical mixing.

WALLACE S. BROECKER
YUAN HUI LI
JOHN CROMWELL
Lamont Geological Observatory,
Columbia University,
Palisades, New York

References and Notes

1. W. S. Broecker, in *Symposium on Diffusion in Oceans and Fresh Waters*, T. Ichite, Ed. (Lamont Geological Observatory, Palisades, N.Y., 1964), pp. 116–145.
2. F. F. Koczy, in *Natural Radium as a Tracer in the Ocean* (U.N. Int. Conf. Peaceful Uses of Atomic Energy) (United Nations, Geneva, 1958), vol. 18, p. 351.
3. ——— and B. Szabc, *J. Oceanogr. Soc. Japan*, 20th anniversary volume (1962); H. Pettersson, *Papers in Marine Biology and Oceanography* [suppl. to *Deep-Sea Res.* **3** (1955)], p. 335; Y. Miyake and Y. Sigimura, *Studies on Oceanography* (Editorial Comm. for Sugawara festival vol., Nagoya, Japan, 1964), p. 274.
4. W. S. Broecker, R. Gerard, W. H. Ewing, B. C. Heezen, *J. Geophys. Res.* **65**, 2903 (1960).
5. T. J. Chow and E. D. Goldberg, *Geochim. Cosmochim. Acta* **20**, 192 (1960).
6. G. S. Bien, N. W. Rakestraw, H. E. Suess, *Bull. Inst. Oceanogr. Monaco* **61**, No. 1278 (1963); *Nuclear Geophysics* (Nat. Acad. Sci.–Nat. Res. Counc. publ. 1075, 1963), p. 152.
7. W. H. Munk, *Deep-Sea Res.* **13**, 707 (1966).
8. D. Lal, E. D. Goldberg, M. Koide, *Science* **131**, 332 (1960).
9. R. Gerard and M. Ewing, *Deep-Sea Res.* **8**, 298 (1961).

10. Supported by Atomic Energy Commission contracts AT(30-1)2493 and AT(30-1)2663. We appreciate the help of F. Gwinner and G. Parker in constructing and maintaining the apparatus. Only because of the help and cooperation of many members of the staff connected with the operation of the Lamont research vessels *Vema* and *Conrad* could these measurements have been carried out. Lamont Geological Observatory contribution No. 1129.

23 August 1967

■

Silica in Alkaline Brines

Abstract. *Analysis of sodium carbonate-bicarbonate brines from closed basins in volcanic terranes of Oregon and Kenya reveals silica contents of up to 2700 parts per million at* pH*'s higher than 10. These high concentrations of* SiO_2 *can be attributed to reaction of waters with silicates, and subsequent evaporative concentration accompanied by a rise in* pH*. Supersaturation with respect to amorphous silica may occur and persist for brines that are out of contact with silicate muds and undersaturated with respect to trona; correlation of* SiO_2 *with concentration of Na and total* CO_2 *support this interpretation. Addition of more-dilute waters to alkaline brines may lower the* pH *and cause inorganic precipitation of substantial amounts of silica.*

The SiO_2 content of natural waters that are not associated with areas of geothermal activity very rarely exceeds 100 parts per million (ppm) (*1*). Commonly accepted saturation values with respect to amorphous silica at 25°C and a *p*H lower than 9.2 are 110 to 140 ppm (*2*). Some chert deposits are thought to have formed by inorganic precipitation of silica (*3*). In recent studies of alkali carbonate brines of a number of closed basins we have encountered waters having exceptionally high silica contents—up to 2700 ppm. These data suggest a simple mechanism for the inorganic precipitation of chert.

Silica contents of brines from four closed basins, three of which belong to the Great Basin province of the western United States, have been plotted against *p*H (Fig. 1), Na (Fig. 2), and total CO_2 when sufficient sample was available (Fig. 3). Silica was determined colorimetrically as the β-silicomolybdate complex (*4*). We have paid special attention to *p*H control and elimination of reductants, and have used tartaric acid to eliminate phosphate interference (*5*). All analyses were repeated several times and checked against synthetic brines of similar composition. Interference by boron or fluoride was negligible. Exceptionally high values of SiO_2 were checked by gravimetric and fusion procedures.

Brines were stored in polyethylene bottles and filtered under pressure through 0.45-μ membranes prior to analysis, although filtration through pore sizes down to less than 0.1 μ showed no effect on silica content. Precipitation of silica during storage was checked by digestion of the complete bottles of duplicate samples. Differences were usually less than 5 percent of the silica content at high concentrations of SiO_2, and much less at low concentrations.

The western Great Basin has several intermontane areas of interior drainage in igneous rock terranes. Most of these basins contain saline lakes or playas with brines high in carbonate; the brines have been derived principally by evaporative concentration. Sodium and carbonate are the dominant ions in solution because alkaline-earth carbonates precipitate, and sources of sulfate or chloride are lacking.

Abert Lake of south-central Oregon, with an area of about 130 km^2, is one of several highly saline remnants of the large pluvial lakes that once occupied the western Great Basin (*6*). The present lake has no outlet, and its level and total surface area reflect the long-term balance between inflow, principally the Chewaucan River, and loss of water by evaporation. Sodium, carbonate species, and chloride ions comprise over 90 percent of the dissolved constituents in Abert Lake and associated springs. In addition to waters from Abert Lake itself, and interstitial solutions from associated lacustrine sediments, we have included a sample from a brine pond on the salt flats at the north end of the